ZaferanTwin: An IoT-Based Digital Twin for Programmed Indoor Flowering and Quality-Preserving Drying of Saffron (*Crocus sativus* L.)

Prasun Chowdhury[1*]

[1]*Department of Electronics and Communication Engineering, St. Thomas' College of Engineering and Technology, Kolkata, West Bengal, India.*

*Corresponding author: Prasun Chowdhury, Department of Electronics and Communication Engineering, St. Thomas' College of Engineering and Technology, 4 Diamond Harbour Road, Kidderpore, Kolkata 700023, West Bengal, India.

E-mail: prasun.chowdhury@stcet.ac.in | Tel.: **+91-9748633833**

Accepted Manuscript/Pre-publication version

Abstract

Saffron is the most expensive spice in the world and its value depends on two temperature-sensitive stages, flower formation in the dormant corm and drying of the stigma, yet earlier Internet of Things systems apply fixed thresholds to a single stage and none links the production record to the final pack. ZaferanTwin, the Internet of Things digital twin that controls both stages in a closed loop and binds their records to each retail pack. A forecast-aware predictive incubation chamber, a dryer with a moisture soft sensor and adaptive schedule, low-power long-range field nodes and a hash-chained ledger were evaluated by simulation under Pampore and Kolkata climates, with sensitivity analyses. Compared with the threshold control of recent saffron greenhouse work, the predictive controller held the chamber within one degree of target, used 27 to 44 percent less heating and cooling energy, removed all rot-favourable hours and narrowed the flowering spread from eight days to six; passive storage in Kolkata produced no flowers. Compared with published fixed-temperature drying, adaptive drying matched the best crocin retention within about one percentage point in a quarter of the time with 43 percent less energy and kept every batch within the permitted moisture range. The cooperative-owned design pays back in 1.4 seasons (1.0 to 2.8 under single-assumption changes), gives smallholders access to Grade I and provenance premiums, creates paid, skilled work for women and allows saffron to be grown outside traditional belts, supporting several Sustainable Development Goals.

Keywords: *Crocus sativus*; Crocin retention; LoRaWAN; Corm incubation; Predictive control; Traceability

Introduction

Problem statement

Saffron is the dried red stigma of the saffron crocus (*Crocus sativus* L.), a sterile triploid geophyte that is multiplied only through daughter corms and harvested entirely by hand (Gresta et al., 2008; Cardone et al., 2020). A kilogram of spice represents well over one hundred thousand flowers picked within a short autumn window (Kumar et al., 2009; Kothari et al., 2021). The commercial value of the spice rests on three apocarotenoids: crocin esters that give colour, picrocrocin that gives bitterness, and safranal that gives aroma (Gohari et al., 2013; Kiani et al., 2018). Under ISO 3632 the colour is graded through the specific absorbance of an aqueous extract at 440 nm, and that value weighs heavily in the commercial class of a lot (Kiani et al., 2018; García-Rodríguez et al., 2017).

Two temperature-governed stages decide most of this value. During summer dormancy the corm forms its flower primordia, and controlled-environment work has shown that storage near 23 to 27 °C favours floral initiation while a later fall to roughly 15 to 17 °C is needed for the flowers to emerge (Molina et al., 2005). Warm, humid storage also favours corm rot, a disease complex dominated by *Fusarium oxysporum* that is now one of the main causes of yield loss in traditional saffron belts (Gupta et al., 2021). After harvest, the way water is removed from the stigmas shapes the final crocin, picrocrocin and safranal content (Carmona et al., 2005; Gregory et al., 2005; Tong et al., 2015). Slow ambient drying exposes moist tissue to oxidative and enzymatic loss for days, whereas excessive heat breaks crocin esters down quickly; both routes follow temperature-dependent first-order kinetics (Tsimidou & Biliaderis, 1997).

Indoor and soilless saffron removes field risks and permits production away from the classical regions. Early work demonstrated aeroponic and hydroponic growth (Souret & Weathers, 2000), plant-factory trials defined suitable nutrient conductivity (Dewir & Alsadon, 2022), light quality combined with growth regulators raised flowers per corm under indoor conditions (Eftekhari et al., 2023), and soilless media were tested for daughter-corm production (Fallahi et al., 2020). Meanwhile, Internet of Things (IoT) technology now combines low-cost sensors, long-range radio and cloud analytics in agriculture (Tzounis et al., 2017; Ayaz et al., 2019; Farooq et al., 2019), extended by data-driven decision making (Wolfert et al., 2017; Liakos et al., 2018), digital twins of farm objects (Verdouw et al., 2021) and ledgers for food provenance (Kamilaris et al., 2019).

Accepted Manuscript/Pre-publication version

For saffron specifically, the IoT literature is still thin. A greenhouse system that compares sensed temperature, humidity, pH, soil moisture and salinity with fixed thresholds has been reported (Khan et al., 2024), and a framework for monitoring agronomic variables has been proposed without performance data (Kour et al., 2022). Post-harvest research has been carried out with laboratory dryers, infrared units, freeze drying and neural-network models (Acar et al., 2011; Akhondi et al., 2011; Hakimzadeh, 2020), and authenticity has been tested with electronic noses, machine vision and deep learning (Heidarbeigi et al., 2015; Elaraby et al., 2023; Movahhed Ghodsinia, 2023). Table 1 sets these studies against four capabilities that a working saffron hub needs at the same time.

Table 1. Literature survey and research gap

Study	Focus	IoT sensing	Closed-loop control	Post-harvest quality	Traceability	Main gap
Molina et al. (2005)	Temperature control of flower formation	−	±	−	−	Growth-chamber rules, no sensing network
Kumar et al. (2009)	Agronomy review	−	−	±	−	Descriptive; no decision support
Kour et al. (2022)	IoT framework for agronomic variables	±	±	−	±	Conceptual; no performance data
Khan et al. (2024)	IoT greenhouse cultivation	+	±	−		Threshold control; no post-harvest stage
Dewir & Alsadon (2022)	Plant-factory hydroponics (EC levels)	±	±	−	−	Nutrition only; flowering not steered
Eftekhari et al. (2023)	Indoor light quality and growth regulators	−	±	±	−	Manual treatments; no IoT
Fallahi et al. (2020)	Soilless daughter-corm production	−	−	−	−	Open shelter; no environmental control
Carmona et al. (2005)	Drying and ageing effects on constituents	−	±	+	−	Fixed regimes; laboratory only
Gregory et al. (2005)	Drying temperature and air flow	−	±	+	−	No in-line moisture feedback
Hakimzadeh (2020)	ANN model of drying quality		−	+	−	Offline model; not in a control loop
Akhondi et al. (2011)	Thin-layer models, infrared dryer		−	±	−	Curve fitting; no adaptive schedule
Heidarbeigi et al. (2015)	Electronic nose for adulteration	±	−	+	−	Bench instrument; no batch history
Elaraby et al. (2023)	Deep-learning authenticity from images	±	−	+	±	Detects fraud, does not prove origin
Kamilaris et al. (2019)	Blockchain in agri-food chains	−	−	−	+	Generic; no saffron process data
Verdouw et al. (2021)	Digital twins in smart farming	+	±	−	±	Framework; not crop-specific
This study (ZaferanTwin)	Phase-aware incubation, adaptive drying, ledger	+	+	+	+	Simulation evidence; field trial pending

+ addressed; ± partly addressed; − not addressed.

Three gaps emerge from Table 1. Flowering control in the cited work relies on fixed thresholds or manual treatments, so the chamber neither anticipates ambient swings nor follows the two-phase temperature programme that flower formation requires. Drying studies identify good regimes but run them on fixed timers, so batch-to-batch differences in initial moisture and load are left uncorrected. Finally, quality assessment and provenance remain separate from the process record, which leaves the grower unable to prove how a given lot was produced.

Proposed solution

The objective of this study was therefore to design and evaluate ZaferanTwin, an IoT digital twin that (i) programmes corm incubation through a forecast-aware predictive controller, (ii)

Accepted Manuscript/Pre-publication version

steers stigma drying with an in-line moisture soft sensor, and (iii) binds both records to each retail pack, and to package it as a cooperative-owned commercial service aligned with the Sustainable Development Goals (SDGs).

The contribution of this work lies at two levels, which are kept separate in the results. At the level of the individual control strategies, forecast-aware predictive control and moisture-feedback drying are established techniques; here they are adapted to the two-phase temperature programme of saffron flowering and to the crocin-loss behaviour of drying stigmas, and their benefit is quantified against threshold control and fixed timers. At the level of the architecture, the novelty is the integration of both temperature-critical stages in one digital twin that shares a common batch identity and process state: the phenology clock that drives the incubation programme also predicts the flowering peak, which can be used to plan picking labour and dryer capacity, and the incubation and drying records are written to the same hash-chained batch entry that appears on the retail label. Existing agricultural IoT systems monitor or control a single stage (Table 1), and none links the pre-flowering and post-harvest stages through a shared model and record. The simulations in this paper quantify the contribution of the control strategies; the architecture-level functions are specified but have not yet been implemented (Figure 1).

Materials and methods (proposed methodology)

Study setting and architecture

The study was a computational experiment carried out at [institution removed for blind review] in 2026. Two climate scenarios were used. Pampore in Jammu and Kashmir represents a traditional saffron belt with mild summers, and Kolkata in West Bengal represents a warm, humid non-traditional location where corms cannot be stored passively. Hourly ambient temperature and relative humidity for the 127-day dormancy-to-flowering period were generated from seasonal means, diurnal amplitudes and correlated noise representative of each site (Note 1). All results reported in this paper were obtained by simulation; no component of the architecture has yet been built or tested in the field. Figure 1 therefore marks which components were evaluated quantitatively and which are specified in the design but not yet implemented.

The proposed architecture has four layers (Figure 1). Layer 1 holds the physical assets: battery field nodes that log soil moisture and temperature, an incubation chamber built inside a retrofitted 20-ft insulated container with distributed temperature and humidity probes, an

Accepted Manuscript/Pre-publication version

inverter heat pump, a dehumidifier and circulation fans, and a tray dryer fitted with air sensors and load cells. Layer 2 carries data over LoRaWAN for field nodes, which is suited to low-rate, long-range links (Adelantado et al., 2017), over Modbus on RS-485 inside the hub, and over a 4G backhaul that stores and forwards when coverage drops. Layer 3 is an edge computer that runs the digital twin: a thermal model of the chamber, a phenology clock for the corm population, the predictive controller, the drying soft sensor and an anomaly detector that flags rot-favourable conditions and sensor faults. Layer 4 provides the hash-chained batch ledger, QR labels, dashboards with SMS and voice alerts in local languages, and the cooperative's market records.

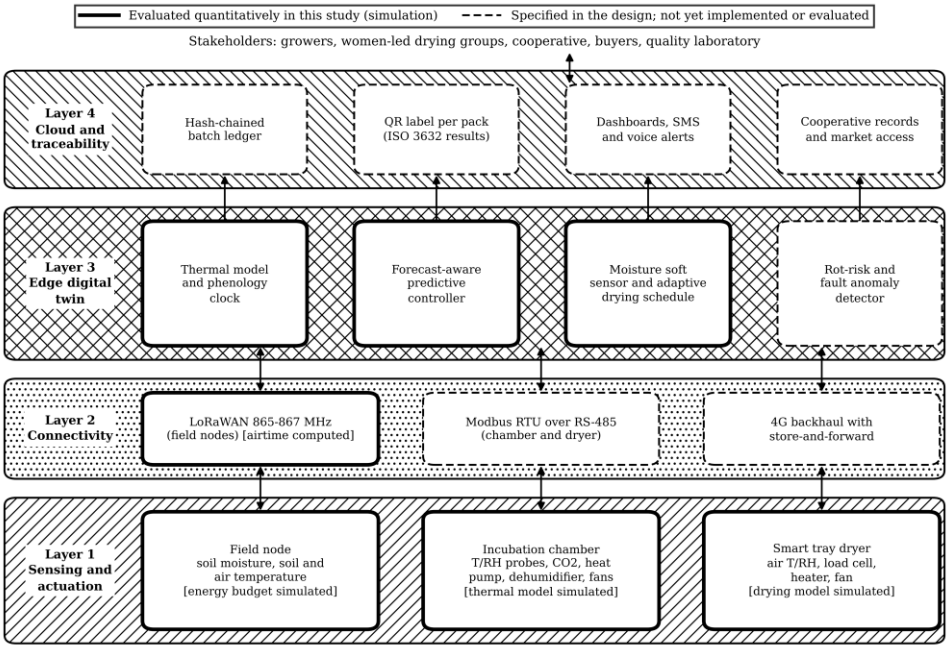

Figure 1. Four-layer architecture of ZaferanTwin. Hatching distinguishes the layers; arrows show data and control flow between the sensing assets, communication links, edge digital twin and cloud services. Boxes with a thick solid border were evaluated quantitatively by simulation in this study; boxes with a dashed border are specified in the design but have not yet been implemented or evaluated.

Incubation chamber model and controllers

The chamber air and the corm mass were lumped into one thermal node, as in Eq. (1):

$$C\frac{dT}{dt} = UA(T_a - T) + Q_{hp} + Q_r \quad (1)$$

where C is the heat capacity of air and corms (J K^{-1}), T the chamber temperature (°C), t time (s), UA the envelope conductance (W K^{-1}), T_a the ambient temperature (°C), Q_{hp} the heat delivered (positive) or removed (negative) by the heat pump (W) and Q_r the respiratory heat of the corms (W). Electrical power was obtained by dividing $|Q_{hp}|$ by a coefficient of performance that falls as the temperature lift grows. Relative humidity followed a first-order balance

Accepted Version

between infiltration, corm transpiration, condensation on the cooling coil and the dehumidifier. Table 2 lists the principal parameters and states, for each, whether it was taken from the literature, assumed or calibrated.

Table 2. Principal model parameters

Parameter	Value	Basis
Chamber heat capacity / envelope conductance	7.0 MJ K-1 / 40 W K-1	A: 20-ft container with 2 t corms
Heat-pump thermal capacity	3.0 kW	A
Phase set-points	25 °C for 90 d, 7-d ramp, 17 °C	L: Molina et al. (2005)
Initiation requirement	90 ± 5 optimal days	L: optimum duration, Molina et al. (2005); A: spread
Initiation rate cardinal temperatures	10 / 25 / 35 °C	L: base and optimum, Molina et al. (2005); A: ceiling
Emergence requirement	18 ± 1 optimal days	A
Emergence rate cardinal temperatures	8 / 17 / 24 °C	L: optimum, Molina et al. (2004, 2005); A: base and ceiling
Corm mass	Lognormal; median 11 g, 5–95 % range 6.7–18.0 g	A: commercial planting stock
Flowering competence	Logistic in mass; 50 % at 7.4 g	C: fitted to Fallahi (2023)
Drying constant at 60 °C, activation energy	0.0621 min-1, 50.4 kJ mol-1	A: Lewis model (Erbay & Icier, 2010)
Crocin loss: wet path k60 / Ea	5.04e-04 min-1 / 20 kJ mol-1	C: rate constant; A: activation energy
Crocin loss: thermal path k60 / Ea	4.56e-03 min-1 / 130 kJ mol-1	C: rate constant; A: activation energy; first order (Tsimidou & Biliaderis, 1997)
Anchor retentions (shade, 40, 60, 80 °C)	80 / 88 / 93 / 90 %	A: ranking from Carmona et al. (2005) and Gregory et al. (2005)
Target moisture (wet basis)	10 % (accept 8-12 %)	A: below ISO 3632 limit
Monte Carlo batches per method	300; 72-86 % initial moisture; load ±20 %	A

L, taken from the literature; A, assumed for this study; C, calibrated within the model. The ranges explored for assumed and calibrated values are given in Table 9.

The temperature programme followed the evidence on flower formation (Molina et al., 2005): 25 °C for 90 days after corm lifting to complete floral initiation, a seven-day linear ramp, and 17 °C until day 127 for emergence. Three strategies were compared. Passive storage left the container unconditioned. The threshold controller, representative of the threshold logic used in earlier saffron IoT work (Khan et al., 2024), switched a fixed-speed compressor at full power whenever the measured temperature left a ±1 °C band and switched the dehumidifier on above 80 % relative humidity. The proposed predictive controller used a 3-h ambient forecast with added error and, every 10 min, chose the heat-pump modulation level u that minimised Eq. (2):

$$J(u) = \sum_{j=1}^{H} \left[w_T \cdot max\left(0, |T_{k+j} - T_{k+j}^{sp}| - \varepsilon\right)^{2} + w_E P_e(u) \right] \quad (2)$$

where H is the horizon (18 steps), $\hat{T}$ the predicted chamber temperature, T_{sp} the phase set-point, ε a 0.6 °C tolerance within which no tracking penalty applies, P_e the electrical power at modulation u, and w_T and w_E weights for tracking and energy. The tolerance lets the chamber ride on its thermal mass, and the forecast lets it pre-condition before the ambient turns against

Accepted Manuscript/Pre-publication version

it. Its dehumidifier target was 74 %, kept below the 80 % level used to define rot-favourable hours.

Phenology and flowering

Flower development was represented with a beta temperature-response function for each sub-phase (Eq. 3):

$$r(T) = \left(\frac{T-T_b}{T_o-T_b}\right)\left(\frac{T_c-T}{T_c-T_o}\right)^{\frac{T_c-T_o}{T_o-T_b}}, \quad T_b < T < T_c \tag{3}$$

where r is the development rate (fraction of the optimal-day requirement per day), T_b, T_o and T_c are the base, optimum and ceiling temperatures (10, 25 and 35 °C for initiation; 8, 17 and 24 °C for emergence). A population of 2,000 corms was simulated. Each corm received its own requirement (90 ± 5 optimal days for initiation, 18 ± 1 for emergence) and a positional temperature offset whose standard deviation reflected air mixing (1.5 °C for passive storage, 1.2 °C for threshold control and 0.4 °C for the predictive controller, which also cycles the fans on stratification readings). A corm flowered on the day its accumulated emergence rate reached its requirement. Outcomes were the share of corms flowered by day 127 and the spread between the 10th and 90th percentiles of flowering date, which sets the length of the picking peak.

These phenological parameters were revised to follow Molina et al. (2005) more closely. In that study, incubation at 23 to 27 °C for more than 50 days was needed for the maximum number of flowers, and incubation beyond 150 days caused flowers to abort; the initiation requirement was therefore set at 90 optimal days, which matches both the optimum duration reported there and the length of the warm phase of the programme. The base temperature for initiation (10 °C) reflects the absence of flower formation at 9 °C, and the optimum (25 °C) lies within the 23 to 27 °C range. Because flowers still formed to a considerable extent at 30 °C, the ceiling was set at 35 °C, which gives a rate at 30 °C of about 84 % of the optimum rate. For emergence, the optimum of 17 °C follows Molina et al. (2004, 2005). Direct evidence on the minimum temperature for emergence is scarce, and shoot growth has been observed from 1 to 30 °C (Molina et al., 2004); a base of 8 °C was therefore assumed and values from 5 to 12 °C were tested. In a chamber held at 17 °C these values do not affect emergence, because the rate equals one at the optimum; they matter only for passive storage.

Corm size was also included, because the reserves stored in the corm determine whether it can flower at all. Under controlled conditions, no corms of 2 to 4 g flowered, whereas 11.2, 38.7 and 85 % of corms of 4 to 6, 6 to 8 and 8 to 10 g did (Fallahi, 2023); larger mother corms

Accepted Manuscript/Pre-publication version

also produce more flowers (Douglas et al., 2014), and corms of 22 to 25 mm diameter did not bloom in hydroponic culture (Dewir et al., 2022). Each simulated corm therefore received a mass drawn from a lognormal distribution representing commercial planting stock (median 11 g, mean 11.4 g, 5 to 95 % range 6.7 to 18.0 g), and a probability of being flowering-competent given by a logistic function of mass fitted to the data of Fallahi (2023), with 50 % competence at 7.4 g. Corms that were not competent did not flower at any temperature. Effects of reserves on the number of flowers per corm and on the rate of development were not modelled. Flowering was reported as a share of all corms and as a share of flowering-competent corms.

Drying model and adaptive schedule

Thin-layer drying was described by the Lewis model, which belongs to the semi-empirical family widely fitted to saffron and other food products (Erbay & Icier, 2010; Akhondi et al., 2011), as in Eq. (4):

$$\frac{dX}{dt} = -k(X - X_e), \;\; k = k_{60} \cdot exp\left[-\frac{E_d}{R}\left(\frac{1}{T_a} - \frac{1}{333.15}\right)\right] \tag{4}$$

where X is the dry-basis moisture content (kg kg^{-1}), X_e the equilibrium moisture (0.06 kg kg^{-1}), k the drying constant (min^{-1}), k_{60} its value at 60 °C, E_d the activation energy (J mol^{-1}), R the gas constant (8.314 J mol^{-1} K^{-1}) and T_a the air temperature (K). Shade drying in still air was assigned one quarter of the forced-air constant. While the tissue is wet it stays close to the wet-bulb temperature, so product temperature was estimated by Eq. (5):

$$T_p = T_a - (T_a - T_{wb})\,\frac{X}{X + 0.4} \tag{5}$$

where T_p is the product temperature and T_{wb} the wet-bulb temperature of the heated air (°C). Crocin loss was modelled as the sum of a moisture-dependent path that dominates during slow drying and a thermal path that dominates at high temperature, each first order (Tsimidou & Biliaderis, 1997), as in Eq. (6):

$$\frac{dC_r}{dt} = -\left[k_w \frac{X}{X + 0.6} + k_t\right] C_r \tag{6}$$

where C_r is the fraction of crocin retained and k_w and k_t are rate constants with Arrhenius dependence on T_p (activation energies 20 and 130 kJ mol^{-1}). The two rate constants were fitted by least squares toward anchor retentions of 80, 88, 93 and 90 % for nominal batches dried in shade and at 40, 60 and 80 °C; the fitted model returned 79, 96, 95 and 89 %, keeping the ordering except that 40 and 60 °C became nearly equal. The anchors are assumptions that encode the ranking reported experimentally, in which brief warm-air dehydration preserves

Accepted Manuscript/Pre-publication version

colour better than slow ambient drying while excessive heat is harmful (Carmona et al., 2005; Gregory et al., 2005; Tong et al., 2015); they are not measured values.

Two limitations of this calibration should be stated. First, the fitted model does not reproduce the 40 °C anchor: it returns 96 % instead of 88 %. With a moisture-driven loss whose rate depends only weakly on temperature, the 3.7 h needed at 40 °C is too short to remove 12 % of the crocin while the 40 h of shade drying still removes about 21 %; meeting both anchors at once would require a loss mechanism that is most active at intermediate temperatures, which the two-path structure does not contain. To show how far the conclusions depend on this choice, the model was refitted in three further ways: with the 40 °C anchor enforced (weight 25 and a free activation energy for the wet path), and with thermal activation energies of 100 and 160 kJ mol^{-1}; for each refit the adaptive schedule was re-optimised. Second, only crocin was modelled. Picrocrocin and safranal also define ISO 3632 quality; safranal forms from picrocrocin during drying and increases at higher drying temperatures (Gregory et al., 2005; del Campo et al., 2010), so a short high-temperature phase such as that of the adaptive schedule may raise safranal, but this was not quantified.

Fixed regimes ran on timers set for a nominal 80 % (wet basis) batch to reach 10 % moisture. The adaptive schedule held a high inlet temperature while the stigmas were wet and protected by evaporative cooling, then lowered it linearly as moisture fell, and stopped when the load-cell estimate of moisture reached 10 %. The load-cell estimate carried 2 % noise. A grid search over the high and low temperatures and the switching moisture selected 85 °C, 47.5 °C and 0.8 kg kg^{-1}. Each method was run on 300 Monte Carlo batches with initial moisture drawn between 72 and 86 % and tray load varied by ±20 %. Colouring strength was obtained by multiplying a batch potential of 240 ± 18 absorbance units by the retained fraction, and the share of batches reaching 190, the colouring-strength threshold of the top ISO 3632 category, was recorded. The fixed regimes therefore represent a dryer operated by a time recipe without moisture measurement, and the comparison measures the value of moisture feedback as well as that of the temperature schedule. A robustness analysis of 1,000 scenarios then varied initial moisture (65 to 90 %), batch load (50 to 150 % of nominal) and all kinetic parameters jointly (drying constant and its activation energy ±20 %, crocin rate constants with a lognormal factor of standard deviation 0.3, wet-path and thermal activation energies ±5 and ±15 kJ mol^{-1}), without re-tuning the adaptive schedule or the timers.

Accepted Manuscript/Pre-publication version

Sensor-node energy and data integrity

Field nodes were budgeted for one 24-byte report every 10 min. LoRa airtime was computed for spreading factors 7 to 12 at 125 kHz bandwidth and coding rate 4/5. Charge per report included transmission at 44 mA, two receive windows at 11.5 mA, sensing and processing, and sleep current was 3.5 µA. Battery life, L in years, followed Eq. (7):

$$L = \frac{Q_b}{8760 \cdot \bar{I}}, \quad \bar{I} = \frac{q + I_s(\tau - t_a)}{\tau} \tag{7}$$

where Q_b is the usable capacity of two AA cells (2,080 mAh), q the charge per report (mC), I_s the sleep current, τ the reporting period (s), t_a the active time (s) and 8,760 the number of hours in a year. A Wi-Fi node that connects and publishes for 2 s per report was evaluated for comparison. Each finished batch record (incubation log digest, drying trace digest, laboratory results and the previous record's hash) is hashed with SHA-256 and the hash is printed as a QR code, so that any later alteration of the record breaks the chain (Kamilaris et al., 2019).

Commercial design and analysis

A cooperative hub was costed from indicative 2026 component prices, and seasonal benefits were estimated from the simulated outcomes under stated price assumptions (Note 2). The Grade I benefit assumes that the cooperative currently dries in the shade, the reference practice in Table 4. The simple payback was recalculated with each of eight economic assumptions varied alone, and with all unfavourable values applied together. All simulations were written in Python 3 with NumPy and SciPy (Note 3).

Sensitivity analysis

Parameters that were assumed or calibrated (Table 2) were varied to test whether the conclusions depend on them. For the chamber, envelope conductance and heat capacity were changed by ±25 %, the forecast error was doubled, the inverter part-load gain was reduced from 25 to 10 %, and the compressor start-up loss was removed; every case reused the same weather and noise sequence, so differences arise from the parameter alone. For flowering, the initiation requirement (60, 90 and 120 days), the initiation ceiling (31, 35 and 38 °C), the emergence base temperature (5, 8 and 12 °C) and the corm stock were varied. The drying and economic analyses are described above.

Accepted Manuscript/Pre-publication version

Results and discussion

Incubation control and flowering

Figure 2 traces the Kolkata scenario. Passive storage left the corms between 28 and 32 °C for the whole period, above the ceiling temperature for floral initiation. Both active controllers held the programme closely, but the threshold controller oscillated across most of its band while the predictive controller stayed in a narrow corridor slightly above the set-point and modulated instead of cycling.

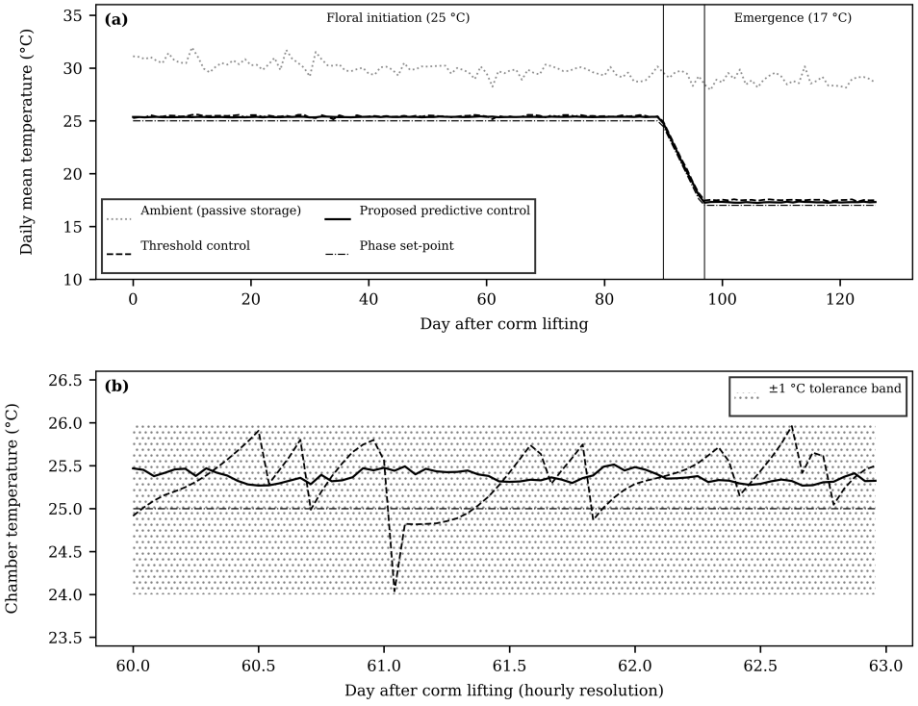

Figure 2. Incubation chamber temperature in the Kolkata scenario: (a) daily means over the 127-day programme for passive storage, threshold control and the proposed predictive control; (b) hourly detail for days 60 to 63 with the ±1 °C tolerance band.

Table 3 summarises chamber performance. At Pampore, the predictive controller kept the chamber within ±1 °C for 100 % of the time and lowered root-mean-square error from 0.42 to 0.33 °C, while thermal energy fell from 116 to 65 kWh, a 44 % saving. The saving came from three sources: inverter part-load efficiency, the absence of start-up losses, and the use of cool nights to bank cooling in the corm mass before warm afternoons. At Kolkata, thermal energy fell by 27 % (400 to 290 kWh). The tighter humidity target raised dehumidifier energy from 358 to 475 kWh, so total consumption was almost unchanged (758 versus 766 kWh). In exchange, rot-favourable hours, defined as chamber temperature above 20 °C with relative humidity above 80 %, fell from 82 h to zero. Given the losses that corm rot inflicts (Gupta et al., 2021), that trade appears favourable, and a lower dehumidifier setting remains available

Accepted Manuscript version

where rot pressure is low. The size of these savings depends on assumed chamber properties; its range is reported in Table 9.

Table 3. Incubation chamber performance over 127 days

Site and control	Time within ±1 °C (%)	RMSE (°C)	Thermal energy (kWh)	Dehumidifier energy (kWh)	Rot-risk hours (h)	Corms flowered, % of all (of competent)	Emergence spread P10-P90 (d)
Pampore: Passive storage	48.4	2.38	0	0	0	57.5 (66.2)	11
Pampore: Threshold control	99.8	0.42	116	0	0	86.0 (99.0)	8
Pampore: Predictive control (proposed)	100.0	0.33	65	0	0	86.8 (99.9)	6
Kolkata: Passive storage	0.0	8.81	0	0	3044	0.0 (0.0)	–
Kolkata: Threshold control	99.2	0.54	400	358	82	86.0 (99.0)	8
Kolkata: Predictive control (proposed)	100.0	0.36	290	475	0	86.7 (99.8)	6

Rot-risk hours: chamber temperature above 20 °C with relative humidity above 80 %. Spread: days between the 10th and 90th percentile of flowering date. Flowering is given as a percentage of all corms, with the percentage of flowering-competent corms in brackets; revised phenological parameters (Table 2).

Flowering outcomes appear in Figure 3. With the commercial corm stock, 86.9 % of corms were large enough to be flowering-competent, which caps flowering in every scenario. Passive storage at Kolkata produced no flowers because the corms never cooled into the emergence window, which explains why saffron cannot simply be relocated to warm lowlands. At Pampore, passive storage brought only 66.2 % of competent corms (57.5 % of all corms) to flower by day 127, spread over 11 days. Both controlled chambers brought 99 to 100 % of competent corms to flower, and the predictive controller narrowed the 10th-to-90th percentile spread from 8 to 6 days because better air mixing reduced the temperature differences between crates. A compact flowering peak lets a cooperative plan pickers, separation labour and dryer capacity around a few predictable days. The total number of flowers depends as much on the corm stock as on temperature control: with ungraded stock (median 8.5 g) the chamber brought only 62.5 % of all corms to flower, and with small stock (median 6 g) 29.5 % (Table 9).

Accepted Manuscript/Pre-publication version

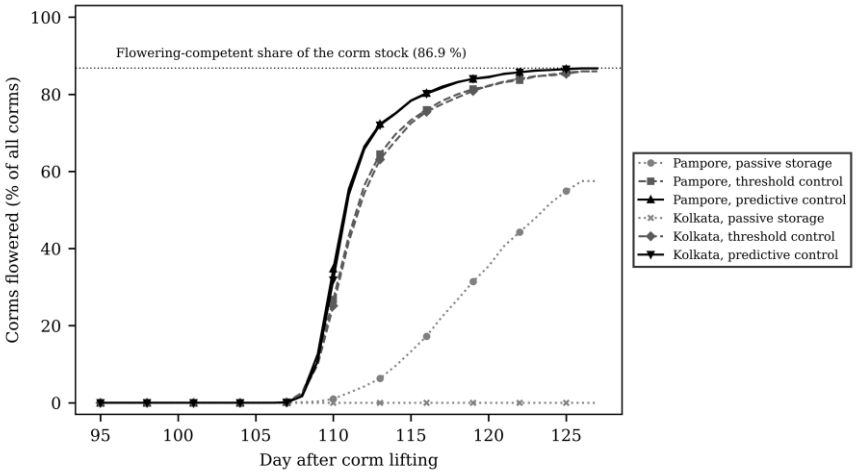

Figure 3. Cumulative share of the 2,000 simulated corms (commercial stock, median mass 11 g) that flowered under each storage strategy at Pampore and Kolkata, with the revised phenological parameters; the dotted line marks the flowering-competent share of the stock (86.9 %).

Stigma drying

Figure 4 shows moisture and crocin trajectories for a nominal batch. Shade drying needed about 40 h and lost crocin steadily throughout. Drying at 80 °C was the fastest but crocin fell sharply in the final minutes, once evaporative cooling no longer protected the tissue. The adaptive schedule followed the fast route while the stigmas were wet and then eased the temperature, so it finished in about an hour without the late thermal loss.

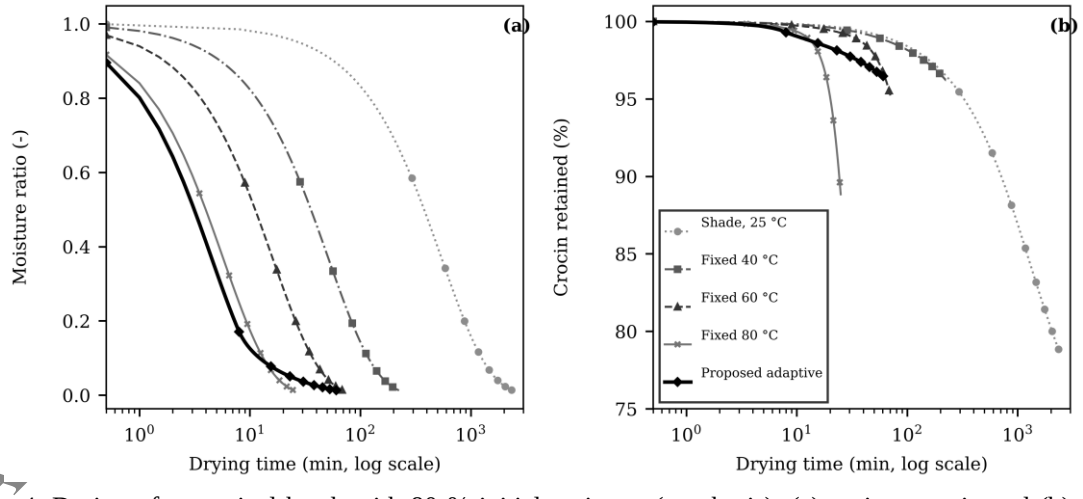

Figure 4. Drying of a nominal batch with 80 % initial moisture (wet basis): (a) moisture ratio and (b) crocin retained against time for shade drying, fixed-temperature regimes and the proposed adaptive schedule.

Table 4 shows that the adaptive schedule matched the best fixed regime in quality and outperformed every fixed regime in consistency. Crocin retention averaged 96.5 %, practically the same as drying at 40 °C (96.2 %) and higher than 60 °C (95.1 %), 80 °C (87.8 %) and shade drying (79.0 %). Compared with 40 °C, it reached that quality in 60 instead of 224 min and with 43 % less energy per kilogram of fresh stigma. The largest difference concerned final

Pre-publication version

moisture. Timers cannot see batch-to-batch differences, so between 36.7 and 42.7 % of fixed-regime batches finished outside the 8 to 12 % window; under-dried lots risk mould and over-dried lots lose saleable mass and become brittle. Feedback from the load cells kept every adaptive batch within the window, with a standard deviation of 0.14 percentage points. In colour terms, 99.0 % of adaptive batches reached a colouring strength of 190, against 46.7 % for shade drying. These comparisons rest on the base calibration. Under the alternative calibrations (Table 9) the difference in retention between the adaptive schedule and drying at 40 °C ranged from −0.8 to +0.7 percentage points, so the schedule should be regarded as matching, not exceeding, the best fixed regime in crocin retention; its time and energy advantages (54 to 64 min and 1.58 to 1.73 kWh kg^{-1}, against 224 min and 2.88 kWh kg^{-1}) were present under every calibration.

Table 4. Drying performance over 300 Monte Carlo batches

Drying method	Time (min)	Final moisture, w.b. (%)	Batches outside 8-12 % (%)	Crocin retained (%)	Colouring strength E1% 440 nm	Batches ≥ 190 (%)	Energy (kWh kg-1 fresh)
Shade drying, 25 °C	2371	10.1 ± 2.39	42.7	79.0 ± 1.71	190	46.7	0.00
Fixed 40 °C, timer	224	10.0 ± 2.22	40.0	96.2 ± 0.04	230	98.3	2.88
Fixed 60 °C, timer	70	10.2 ± 2.32	36.7	95.1 ± 0.97	229	99.3	2.02
Fixed 80 °C, timer	25	10.1 ± 2.33	41.7	87.8 ± 4.06	211	87.0	1.11
Adaptive schedule (proposed)	60	10.1 ± 0.14	0.0	96.5 ± 0.41	231	99.0	1.63

Values are mean ± standard deviation over 300 batches. Colouring strength is the absorbance E1% 1 cm at 440 nm; 190 is the threshold of the top ISO 3632 category.

Network energy

Table 5 confirms that the low-rate LoRaWAN link is the appropriate choice for field nodes. At spreading factors 7 and 9 the average current stayed near 10 to 21 µA, giving a nominal battery life beyond 10 years, so cell shelf life rather than radio use sets the replacement interval. Even at spreading factor 12, needed for the most distant plots, two AA cells lasted about 1.9 years. A Wi-Fi node with the same reporting period would need new batteries roughly every seven months, which is impractical across scattered smallholdings.

Table 5. Sensor-node energy budget, one report every 10 min

Radio configuration	Air or active time (ms)	Charge per report (mC)	Average current (µA)	Battery life, 2 × AA (years)
LoRaWAN SF7	62	3.6	9.5	≥ 10 (shelf-life bound)
LoRaWAN SF9	206	10.5	21.0	≥ 10 (shelf-life bound)
LoRaWAN SF10	371	18.5	34.3	6.92
LoRaWAN SF12	1483	71.9	123.4	1.92
Wi-Fi node	2000	240.4	410.6	0.58

Superiority and novelty with respect to recent literature

Table 6 places these results beside the most closely related studies. Two cautions apply. The comparison is partly qualitative, because the earlier saffron IoT system did not report

Accepted Manuscript/Pre-publication version

energy or yield figures (Khan et al., 2024); its logic was therefore reproduced as the threshold baseline so that both controllers faced identical weather. In addition, the present results are simulated, with several kinetic and economic parameters assumed, so they establish relative performance under controlled conditions rather than field-verified absolute values.

Table 6. Superiority and novelty of ZaferanTwin relative to recent literature

Reference study	Reported capability	ZaferanTwin result (this study)
Khan et al. (2024): threshold IoT control	Threshold actuation of temperature and humidity; no numeric yield or energy result reported	Against a threshold baseline: thermal energy −44 % (Pampore) and −27 % (Kolkata); rot-risk hours 82 → 0
Kour et al. (2022): IoT framework for saffron agronomic variables	Sensing and control architecture proposed; no performance data reported	Quantified control performance (energy, tracking, rot-risk, flowering) and an added post-harvest stage
Molina et al. (2005): temperature windows	Optimal storage temperatures for flower formation identified in chambers	Windows held within ±1 °C for 100 % of time at both sites; flowering spread 8 → 6 d; 99.9 % of flowering-competent corms flowered
Eftekhari et al. (2023): indoor flowering	Up to 1.97 flowers per corm under red-blue light with growth regulator	Complementary: supplies the temperature programme that such light treatments assume; enables flowering where passive storage gave 0 %
Dewir & Alsadon (2022); Dewir et al. (2022): plant-factory and hydroponic saffron	Nutrient conductivity and corm size shape flowering and yield	Complementary: supplies programmed incubation and corm-stock-aware flowering prediction for such systems
Carmona et al. (2005); Gregory et al. (2005): fixed drying	Warm-air dehydration preserves colour better than slow ambient drying	Retention within about ±1 point of 40 °C drying across calibrations (96.5 vs 96.2 % in the base case) in 27 % of the time and 43 % less energy
Hakimzadeh (2020): ANN drying model	Offline prediction of crocin (R^2 0.914) from temperature, time and layer thickness	Online moisture soft sensor: final moisture SD 0.14 vs 2.22 points; 0 % batches out of 8-12 %
Elaraby et al. (2023); Heidarbeigi et al. (2015): authenticity	99 % image accuracy; electronic-nose discrimination of adulterants	Complementary: hash-chained process log binds each pack to its incubation and drying record

Within those limits, the proposed system combines three capabilities that no surveyed study joins. First, it closes the loop on the temperature windows that flower formation requires (Molina et al., 2005), saving energy where the threshold approach wastes it. Second, it turns the established knowledge on drying temperature (Carmona et al., 2005; Gregory et al., 2005) and offline quality models (Hakimzadeh, 2020) into an online schedule that corrects for each batch. Third, it complements authenticity testing (Heidarbeigi et al., 2015; Elaraby et al., 2023) with a verifiable production record, so a buyer scanning a pack sees how that lot was incubated and dried rather than only whether it looks genuine.

Taken together, these comparisons show where ZaferanTwin is superior to earlier solutions and where it is new. It outperformed the threshold logic of the earlier saffron greenhouse system (Khan et al., 2024) on every chamber criterion examined: 27 to 44 % less thermal energy in the reference case (20 to 55 % across the sensitivity cases), complete removal of the 81 to 83 rot-favourable hours that threshold control left in a humid climate, tighter temperature tracking (root-mean-square error 0.33 to 0.36 °C against 0.42 to 0.54 °C) and a flowering peak shortened from 8 to 6 days. Against the fixed drying regimes studied by Carmona et al. (2005), Gregory et al. (2005) and Tong et al. (2015), it reached the best crocin retention in about a quarter of the time and with 43 % less energy, and it was the only method that kept every batch within

Accepted Manuscript/Pre-publication version

the 8 to 12 % moisture window, against 23 to 25 % of timer batches when moisture and load varied. Unlike the offline quality model of Hakimzadeh (2020) and the bench authenticity tests of Heidarbeigi et al. (2015) and Elaraby et al. (2023), it acts online during processing and leaves a verifiable record. Its novelty lies in this combination: to the author's knowledge, no earlier study has steered both flower formation and stigma drying with one digital twin, quantified how the corm stock limits programmed flowering, or bound the incubation and drying records to the retail pack. A retention advantage over the best fixed regime is not claimed, because the sensitivity analysis placed it within the model uncertainty.

Commercial design for social well-being

Figure 5 outlines the commercial design: four tiers that a farmer producer organisation can adopt step by step, namely a leased field kit, the incubator in a retrofitted reefer container, a smart dryer run by a women's self-help group, and the ZT-Trace platform issuing QR labels. Revenue comes from node leases, incubation fees, pay-per-batch drying and a per-gram traceability fee, so smallholders pay for service rather than owning equipment.

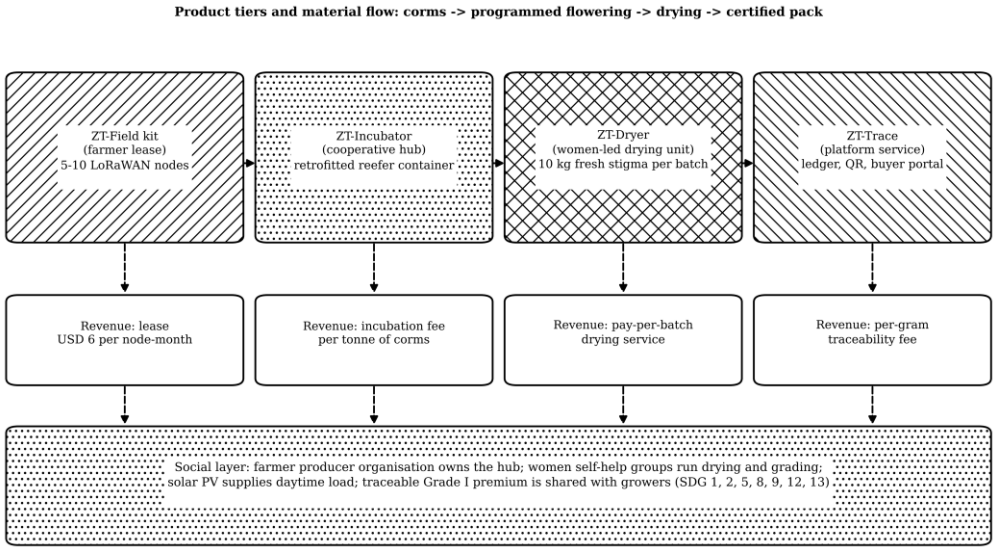

Figure 5. Commercial design of ZaferanTwin: product tiers, material flow, revenue streams and the social layer that links the cooperative hub to the Sustainable Development Goals.

Table 7 shows that one hub costs about USD 15,100. Under the stated assumptions it returns a net benefit near USD 10,550 per season, giving a simple payback of about 1.4 seasons. Almost all of the benefit comes from quality: the move of about 21 kg per season into the top colour class and a modest traceability premium. Extra flowering from incubation contributes far less, so the investment case does not depend on the most uncertain biological assumption. A 3 kWp photovoltaic array covers the daytime load, keeping operating cost low and limiting

Accepted manuscript, publication version

exposure to unreliable rural grids. Because these figures rest on assumed prices, premiums and throughput, their sensitivity is examined below (Figure 6c).

Table 7. Commercial hub cost and seasonal economics

Item	Value (USD)	Note
Incubator: used 20-ft reefer shell, inverter heat pump, dehumidifier, racks, sensors and gateway	7,800	Capital cost, indicative 2026 prices
Two smart tray dryers with load cells	3,200	Capital cost, indicative 2026 prices
Twenty LoRaWAN field nodes and 3 kWp solar PV	4,100	Capital cost, indicative 2026 prices
Total capital cost of one cooperative hub	15,100	Serves about 150 growers
Benefit: Grade I upgrade	5,233	20.9 kg moved to ≥190 class at USD 250 kg-1
Benefit: traceability premium	5,000	5 % on 40 kg at USD 2,500 kg-1
Benefit: extra flowering from incubation	1,188	73,125 extra flowers at 6.5 mg each (revised phenology)
Operating cost per season	876	Maintenance 4 %, platform, labels, grid share of 392 kWh
Net benefit per season	10,546	Simple payback 1.4 seasons

Indicative values in US dollars; assumptions in Note 2.

Table 8 maps the design to the SDGs. The strongest links are to SDG 1 and SDG 12, through premiums returned to growers and fewer downgraded or re-dried lots. Much of the picking and stigma separation is done by women in many producing regions, so giving women's groups paid, skilled roles in drying and grading supports SDG 5. Decoupling flowering from warming summers is an adaptation measure under SDG 13. Each mechanism is tied to an indicator that the platform already logs, so social outcomes can be reported alongside technical ones.

Table 8. Mapping of the commercial design to the SDGs

SDG	ZaferanTwin mechanism	Indicator tracked by the platform
SDG 1 No poverty	Grade I and traceability premiums returned to growers	Farm-gate price per gram by grower
SDG 2 Zero hunger	Higher output per corm and per unit water	Flowers per corm; irrigation events
SDG 5 Gender equality	Women self-help groups operate and are paid for drying and grading	Paid hours and income share of women
SDG 8 Decent work	Shorter, planned harvest peak reduces night picking	Emergence spread (days)
SDG 9 Industry and innovation	Rural IoT and edge computing serviced locally	Hub uptime; local technicians trained
SDG 12 Responsible production	Fewer downgraded and re-dried batches; fraud deterrence	Batches outside moisture window; verified scans
SDG 13 Climate action	Decoupling flowering from warming summers; solar supply	Energy per gram; PV share

Sensitivity, robustness and limitations

Table 9 summarises how the main results respond to the assumed and calibrated parameters. For the incubation chamber, the thermal energy saving of predictive over threshold control ranged from 32 to 55 % at Pampore and from 20 to 36 % at Kolkata across the cases tested. It was most sensitive to the heat capacity of the chamber and corms, which sets how much cooling can be stored overnight, and to the part-load efficiency of the inverter heat pump; doubling the forecast error had almost no effect. In every case the predictive controller kept the chamber within ±1 °C for the whole season and removed all rot-favourable hours, whereas the threshold controller left 81 to 83 h at Kolkata, and total consumption at Kolkata stayed within

Accepted Manuscript/Pre-publication version

±5 % of threshold control. The direction of the result is therefore robust, while its size depends on chamber properties that a pilot unit must measure.

For flowering, the initiation ceiling (31 to 38 °C) and the emergence base temperature (5 to 12 °C) had no material effect inside the controlled chamber, which holds temperatures near the optima. They did change the outcome of passive storage at Pampore, where the share of competent corms flowering by day 127 ranged from 36 % (emergence base 12 °C) to 76 % (5 °C). The initiation requirement mattered more for timing than for the final share: with a fixed 90-day warm phase, a requirement of 120 days delayed the median flowering date to day 149 and widened the spread to 19 days. Because the phenology clock of the twin tracks progress towards initiation, the warm phase can instead be extended to match the requirement; doing so restored a 7-day spread at the cost of a later season (median day 141). The corm stock had the largest effect on the total: grading out corms below 8 g raised flowering in the chamber to 94.3 % of all corms.

For drying, Table 9 compares the four calibrations of the crocin model. Enforcing the 40 °C anchor required a single, strongly temperature-dependent loss path (activation energy 92 kJ mol^{-1}), lowered all predicted retentions and shifted the optimal high temperature from 85 to 80 °C; under it the adaptive schedule retained 89.0 % of crocin against 89.8 % at 40 °C. Thermal activation energies of 100 and 160 kJ mol^{-1} moved the difference to −0.5 and +0.7 points. In the robustness analysis (Figure 6a, b), the median difference in retention against 40 °C drying was +0.5 points (5th to 95th percentile −2.7 to +2.5), and the adaptive schedule was within 0.5 points of 40 °C drying or better in 73 % of scenarios. Its advantage was largest for small batches (median +1.7 points at loads below 80 % of nominal) and reversed slightly for large batches (−0.8 points above 120 %), because a heavy tray stays longer at a high air temperature. Drying time was 27 % (15 to 42 %) and energy 57 % (31 to 89 %) of the 40 °C values, with little dependence on initial moisture. The clearest benefit was moisture control: all adaptive batches finished between 8 and 12 % moisture, against 23 % of 40 °C and 25 % of 60 °C timer batches, which cannot respond to differences in initial moisture or load. The advantages are therefore robust for time, energy and moisture consistency, but not for crocin retention, which should be described as equivalent to that of the best fixed regime.

Accepted Manuscript, Pre-publication version

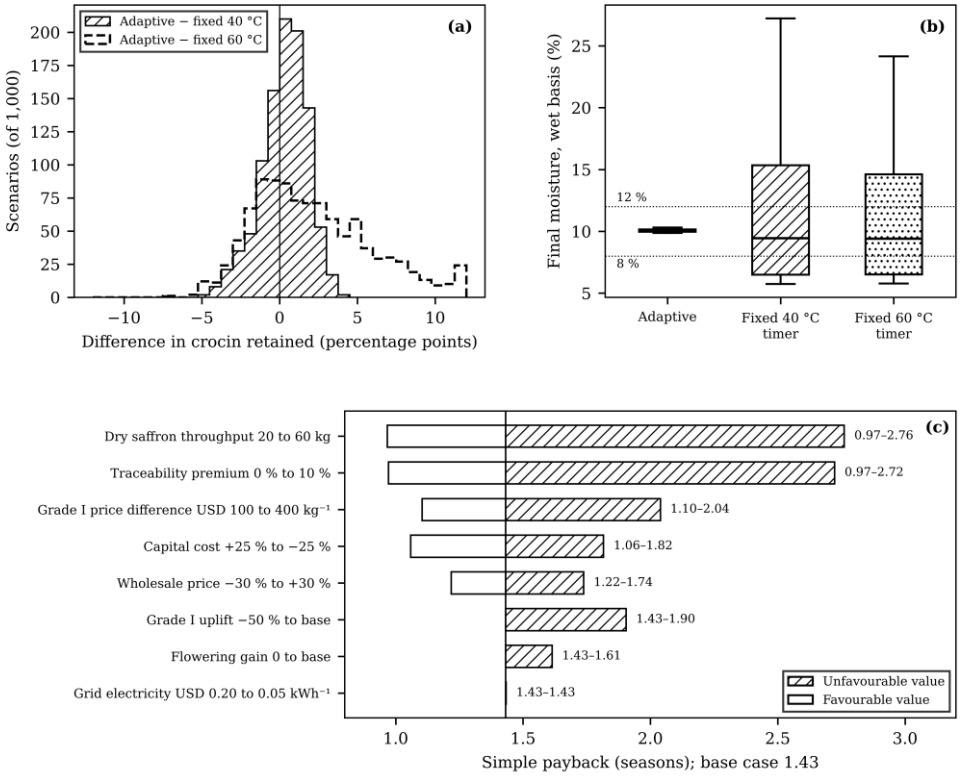

Figure 6. Sensitivity and robustness: (a) difference in crocin retained between the adaptive schedule and fixed 40 °C and 60 °C timers over 1,000 scenarios with varied initial moisture, batch load and kinetic parameters (differences beyond ±12 points are pooled at the edges); (b) final moisture in the same scenarios (boxes, interquartile range; whiskers, 5th to 95th percentiles; dotted lines, the 8 to 12 % target window); (c) simple payback of the cooperative hub when each economic assumption is varied alone.

The economic result was most sensitive to the traceability premium and to throughput (Figure 6c). Without any traceability premium the payback lengthened to 2.7 seasons, and with 20 kg of dry saffron per season to 2.8 seasons; every other single change kept it below 2.1 seasons. Removing the flowering gain altogether changed it only from 1.4 to 1.6 seasons, so the case does not rest on the most uncertain biological assumption. When all unfavourable values were applied together, however, the hub did not recover its operating cost. The economic conclusion therefore holds for a cooperative that can sell at least part of its output with verified provenance or at Grade I prices, and should not be read as a guarantee for every setting.

Finally, the practical claims of this study are bounded by its method. All results are simulated: the thermal, phenological and drying models were evaluated and the LoRaWAN airtime and energy budget were computed, but the ledger, labels, alerts, Modbus and 4G links, rot-risk detector and the integrated operation of the hub were specified and not implemented (Figure 1). The quality predictions rest on assumed anchor retentions rather than on measured samples, and safranal and picrocrocin were not modelled. A pilot hub is therefore planned in which each drying regime is applied to split lots of the same harvest, crocin (E1% at 440 nm),

Accepted Manuscript/Pre-publication

picrocrocin (257 nm), safranal (330 nm) and moisture are measured by ISO 3632 spectrophotometry and confirmed by HPLC (García-Rodríguez et al., 2017), and flowering is recorded for corms weighed individually at lifting. These data will be used to refit the kinetic and phenological parameters in Table 2 before field performance is claimed.

Table 9. Sensitivity of the main results to assumed and calibrated parameters

Parameter varied	Reference case	Result under variation
Envelope conductance UA, ±25 %	Thermal saving 44.1 % (Pampore), 27.4 % (Kolkata)	Pampore 43.7–46.1 %; Kolkata 25.7–28.3 %
Heat capacity of chamber and corms, ±25 %	As above	Pampore 32.1–54.5 %; Kolkata 23.5–36.0 %
Forecast error doubled (σ 1.6 °C)	As above	Pampore 43.9 %; Kolkata 27.4 %
Inverter part-load gain 10 % instead of 25 %	As above	Pampore 38.6 %; Kolkata 19.5 %
No compressor start-up loss	As above	Pampore 39.4 %; Kolkata 22.1 %
All thermal cases above	100 % of time within ±1 °C; rot-risk 0 h (predictive) vs 82 h (threshold, Kolkata)	Unchanged: 100 % within ±1 °C; 0 h vs 81–83 h
Initiation requirement 60 or 120 d, warm phase fixed at 90 d	Median flowering day 111; spread 6 d	Day 110, spread 2 d (60 d); day 149, spread 19 d (120 d)
Initiation requirement 120 d, warm phase extended by the twin	As above	Median day 141; spread 7 d
Initiation ceiling 31 or 38 °C	Chamber 99.9 %; passive Pampore 66.2 % of competent corms	Chamber 99.8–99.9 %; passive Pampore 65.6–66.4 %
Emergence base 5 or 12 °C	As above	Chamber 99.9 %; passive Pampore 75.8 % (5 °C), 36.4 % (12 °C)
Corm stock: ungraded (median 8.5 g), small (6 g), graded ≥ 8 g	Chamber 86.8 % of all corms (median 11 g)	62.5 %, 29.5 %, 94.3 % of all corms
Crocin model with 40 °C anchor enforced	Adaptive 96.5 % vs 40 °C 96.2 %; schedule 85 / 47.5 °C	Adaptive 89.0 % vs 40 °C 89.8 %; schedule 80 / 47.5 °C
Thermal activation energy 100 or 160 kJ mol-1	Difference +0.3 points	−0.5 points (100); +0.7 points (160)
Joint variation of moisture (65–90 %), load (50–150 %) and kinetics; 1,000 scenarios	Single nominal batch	Retention difference +0.5 (−2.7 to +2.5) points; time 27 % (15–42 %) and energy 57 % (31–89 %) of 40 °C; in window 100 % vs 23 % (40 °C) and 25 % (60 °C)
Economic assumptions varied one at a time (Figure 6c)	Payback 1.4 seasons	0.97–2.76 seasons; all unfavourable values together: operating cost not recovered

Values in brackets are 5th to 95th percentiles. Thermal cases reuse the weather and noise sequence of Table 3. Percentages of competent corms are those flowering by day 127.

Conclusion and benefits to society

This study designed ZaferanTwin, an IoT digital twin that joins programmed corm incubation, adaptive stigma drying and a verifiable batch ledger in one cooperative service. In simulations calibrated to published temperature responses and drying behaviour, the predictive incubation controller held the flowering programme within ±1 °C at all times. It cut thermal energy by 27 to 44 % against threshold control, removed rot-favourable hours in a humid climate, enabled flowering where passive storage failed, and narrowed the flowering spread from eight to six days. The adaptive dryer matched the crocin retention of the best fixed regime, to within about one percentage point across alternative calibrations, in about a quarter of the time and kept every batch inside the moisture window, while LoRaWAN field nodes could run for years on two AA cells. The commercial hub appears to pay back within two seasons in the base case, although the payback depends strongly on the traceability premium and throughput,

Accepted Manuscript/Pre-publication version

with benefits that map onto several SDGs. Because the evidence is computational and some parameters are assumed, the next step is a pilot hub in which the chamber, dryer and ledger are built and validated against laboratory measurements of crocin, picrocrocin, safranal and moisture, and against the flowering of individually weighed corms, under real harvest conditions.

The design offers concrete social benefits: smallholders can share a cooperative hub instead of buying equipment and can earn Grade I and provenance premiums; women's self-help groups gain paid, skilled work in drying and grading; a shorter, predictable flowering peak reduces night-time picking; verified batch records protect consumers and honest producers against adulteration; and programmed indoor flowering allows saffron to be grown where warm summers or a warm climate prevent it today. These benefits map onto SDGs 1, 2, 5, 8, 9, 12 and 13 (Table 8).

Conflict of interest

The authors have declared no conflict of interest.

Notes

1. Ambient inputs were synthetic. Pampore used a seasonal mean of 22 °C rising to about 25 °C and easing in autumn, a diurnal amplitude of 7.5 °C and relative humidity near 55 %; Kolkata used a mean of 31 °C easing to 28.5 °C, an amplitude of 4 °C and relative humidity near 82 %. A field study should replace them with station records.

2. Economic assumptions: wholesale price USD 2,500 kg^{-1}; Grade I price difference USD 250 kg^{-1}; traceability premium 5 %; 40 kg of dry saffron per cooperative season from about 200 kg of fresh stigma; 2 t (about 250,000) corms incubated; 6.5 mg of dry stigma per flower; maintenance 4 % of capital per season; grid electricity USD 0.10 kWh^{-1} for the 30 % of demand not met by photovoltaics.

3. The simulation code, generated data and the Excel files behind Figures 2 to 4 are available from the corresponding author on request.

References

Acar, B., Sadikoglu, H., & Ozkaymak, M. (2011). Freeze drying of saffron (*Crocus sativus* L.). *Drying Technology*, *29*(14), 1622–1627. https://doi.org/10.1080/07373937.2011.594378

Accepted Manuscript/Pre-publication version

Adelantado, F., Vilajosana, X., Tuset-Peiro, P., Martinez, B., Melià-Seguí, J., & Watteyne, T. (2017). Understanding the limits of LoRaWAN. *IEEE Communications Magazine, 55*(9), 34–40. https://doi.org/10.1109/MCOM.2017.1600613

Akhondi, E., Kazemi, A., & Maghsoodi, V. (2011). Determination of a suitable thin layer drying curve model for saffron (*Crocus sativus* L.) stigmas in an infrared dryer. *Scientia Iranica, 18*(6), 1397–1401. https://doi.org/10.1016/j.scient.2011.09.012

Ayaz, M., Ammad-Uddin, M., Sharif, Z., Mansour, A., & Aggoune, E.-H. M. (2019). Internet-of-Things (IoT)-based smart agriculture: Toward making the fields talk. *IEEE Access, 7*, 129551–129583. https://doi.org/10.1109/ACCESS.2019.2932609

Cardone, L., Castronuovo, D., Perniola, M., Cicco, N., & Candido, V. (2020). Saffron (*Crocus sativus* L.), the king of spices: An overview. *Scientia Horticulturae, 272*, 109560. https://doi.org/10.1016/j.scienta.2020.109560

Carmona, M., Zalacain, A., Pardo, J. E., López, E., Alvarruiz, A., & Alonso, G. L. (2005). Influence of different drying and aging conditions on saffron constituents. *Journal of Agricultural and Food Chemistry, 53*(10), 3974–3979. https://doi.org/10.1021/jf0404748

del Campo, C. P., Carmona, M., Maggi, L., Kanakis, C. D., Anastasaki, E. G., Tarantilis, P. A., Polissiou, M. G., & Alonso, G. L. (2010). Effects of mild temperature conditions during dehydration procedures on saffron quality parameters. *Journal of the Science of Food and Agriculture*, *90*(4), 719–725. https://doi.org/10.1002/jsfa.3877

Dewir, Y. H., & Alsadon, A. (2022). Effects of nutrient solution electrical conductivity on the leaf gas exchange, biochemical stress markers, growth, stigma yield, and daughter corm yield of saffron in a plant factory. *Horticulturae, 8*(8), 673. https://doi.org/10.3390/horticulturae8080673

Dewir, Y. H., Alsadon, A. A., Ibrahim, A., & El-Mahrouk, M. E. (2022). Effects of growing substrate, mode of nutrient supply, and saffron corm size on flowering, growth, photosynthetic competence, and cormlet formation in hydroponics. *HortTechnology, 32*(2), 234–240. https://doi.org/10.21273/HORTTECH04980-21

Douglas, M. H., Smallfield, B. M., Wallace, A. R., & McGimpsey, J. A. (2014). Saffron (*Crocus sativus* L.): The effect of mother corm size on progeny multiplication, flower and stigma production. *Scientia Horticulturae, 166*, 50–58. https://doi.org/10.1016/j.scienta.2013.12.007

Eftekhari, M., Ghorbani Javid, M., Aliniaeifard, S., & Nicola, S. (2023). Alteration of flower yield and phytochemical compounds of saffron (*Crocus sativus* L.) by application of different light qualities and growth regulators. *Horticulturae, 9*(2), 169. https://doi.org/10.3390/horticulturae9020169

Accepted Manuscript/Pre-publication version

Elaraby, A., Ali, H., Zhou, B., & Fonseca, J. M. (2023). Digging for gold: Evaluating the authenticity of saffron (*Crocus sativus* L.) via deep learning optimization. *Frontiers in Horticulture, 2*, 1225683. https://doi.org/10.3389/fhort.2023.1225683

Erbay, Z., & Icier, F. (2010). A review of thin layer drying of foods: Theory, modeling, and experimental results. *Critical Reviews in Food Science and Nutrition, 50*(5), 441–464. https://doi.org/10.1080/10408390802437063

Fallahi, H. R. (2023). Evaluation of flowering potential of saffron corms in different weight groups under hydroponic conditions. *Journal of Saffron Research, 10*(2), 331–344. [in Persian].

Fallahi, H. R., Abbasi Avval Bahlouli, S., Noferesti, E., Hosseini, S. M., Sadigh Mako, S., Moodi, M., & Khezri, M. (2020). Evaluating the feasibility of saffron corm growth and production in a soilless culture medium. *Journal of Saffron Research, 8*(2), 269–284. https://doi.org/10.22077/jsr.2020.3492.1135 [in Persian].

Farooq, M. S., Riaz, S., Abid, A., Abid, K., & Naeem, M. A. (2019). A survey on the role of IoT in agriculture for the implementation of smart farming. *IEEE Access, 7*, 156237–156271. https://doi.org/10.1109/ACCESS.2019.2949703

García-Rodríguez, M. V., López-Córcoles, H., Alonso, G. L., Pappas, C. S., Polissiou, M. G., & Tarantilis, P. A. (2017). Comparative evaluation of an ISO 3632 method and an HPLC-DAD method for safranal quantity determination in saffron. *Food Chemistry, 221*, 838–843. https://doi.org/10.1016/j.foodchem.2016.11.087

Gohari, A. R., Saeidnia, S., & Mahmoodabadi, M. K. (2013). An overview on saffron, phytochemicals, and medicinal properties. *Pharmacognosy Reviews, 7*(13), 61–66. https://doi.org/10.4103/0973-7847.112850

Gregory, M. J., Menary, R. C., & Davies, N. W. (2005). Effect of drying temperature and air flow on the production and retention of secondary metabolites in saffron. *Journal of Agricultural and Food Chemistry, 53*(15), 5969–5975. https://doi.org/10.1021/jf047989j

Gresta, F., Lombardo, G. M., Siracusa, L., & Ruberto, G. (2008). Saffron, an alternative crop for sustainable agricultural systems. A review. *Agronomy for Sustainable Development, 28*(1), 95–112. https://doi.org/10.1051/agro:2007030

Gupta, V., Sharma, A., Rai, P. K., Gupta, S. K., Singh, B., Sharma, S. K., Singh, S. K., Hussain, R., Razdan, V. K., Kumar, D., Paswal, S., Pandit, V., & Sharma, R. (2021). Corm rot of saffron: Epidemiology and management. *Agronomy, 11*(2), 339. https://doi.org/10.3390/agronomy11020339

Hakimzadeh, V. (2020). Evaluation of modeling the saffron drying process by the pendulum method using an artificial neural network. *Journal of Saffron Research, 8*(1), 115–126. https://doi.org/10.22077/jsr.2020.2749.1111 [in Persian].

Accepted Manuscript/Pre-publication version

595 Heidarbeigi, K., Mohtasebi, S. S., Foroughirad, A., Ghasemi-Varnamkhasti, M., Rafiee, S., & Rezaei,
596 K. (2015). Detection of adulteration in saffron samples using electronic nose. *International*
597 *Journal of Food Properties, 18*(7), 1391–1401. https://doi.org/10.1080/10942912.2014.915850
598 Kamilaris, A., Fonts, A., & Prenafeta-Boldú, F. X. (2019). The rise of blockchain technology in
599 agriculture and food supply chains. *Trends in Food Science & Technology, 91*, 640–652.
600 https://doi.org/10.1016/j.tifs.2019.07.034
601 Khan, R., Farooq, M. S., Khelifi, A., Ahmad, U., Ahmad, F., & Riaz, S. (2024). Internet of things
602 (IoT) based saffron cultivation system in greenhouse. *Scientific Reports, 14*(1).
603 https://doi.org/10.1038/s41598-024-69513-1
604 Kiani, S., Minaei, S., & Ghasemi-Varnamkhasti, M. (2018). Instrumental approaches and innovative
605 systems for saffron quality assessment. *Journal of Food Engineering, 216*, 1–10.
606 https://doi.org/10.1016/j.jfoodeng.2017.06.022
607 Kothari, D., Thakur, R., & Kumar, R. (2021). Saffron (*Crocus sativus* L.): Gold of the spices—a
608 comprehensive review. *Horticulture, Environment, and Biotechnology, 62*(5), 661–677.
609 https://doi.org/10.1007/s13580-021-00349-8
610 Kour, K., Gupta, D., Gupta, K., Juneja, S., Kaur, M., Alharbi, A. H., & Lee, H.-N. (2022). Controlling
611 agronomic variables of saffron crop using IoT for sustainable agriculture. *Sustainability, 14*(9),
612 5607. https://doi.org/10.3390/su14095607
613 Kumar, R., Singh, V., Devi, K., Sharma, M., Singh, M. K., & Ahuja, P. S. (2009). State of art of
614 saffron (*Crocus sativus* L.) agronomy: A comprehensive review. *Food Reviews International,*
615 *25*(1), 44–85. https://doi.org/10.1080/87559120802458503
616 Liakos, K. G., Busato, P., Moshou, D., Pearson, S., & Bochtis, D. (2018). Machine learning in
617 agriculture: A review. *Sensors, 18*(8), 2674. https://doi.org/10.3390/s18082674
618 Molina, R. V., García-Luis, A., Coll, V., Ferrer, C., Valero, M., Navarro, Y., & Guardiola, J. L.
619 (2004). Flower formation in the saffron crocus (*Crocus sativus* L.): The role of temperature. *Acta*
620 *Horticulturae, 650*, 39–47. https://doi.org/10.17660/ActaHortic.2004.650.2
621 Molina, R. V., Valero, M., Navarro, Y., Guardiola, J. L., & García-Luis, A. (2005). Temperature
622 effects on flower formation in saffron (*Crocus sativus* L.). *Scientia Horticulturae, 103*(3), 361–
623 379. https://doi.org/10.1016/j.scienta.2004.06.005
624 Movahhed Ghodsinia, S. R. (2023). Applications of machine vision in the saffron plant field. *Journal*
625 *of Saffron Research, 11*(1), 177–200. https://doi.org/10.22077/jsr.2023.6225.1211 [in Persian].
626 Souret, F. F., & Weathers, P. J. (2000). The growth of saffron (*Crocus sativus* L.) in aeroponics and
627 hydroponics. *Journal of Herbs, Spices & Medicinal Plants, 7*(3), 25–35.
628 https://doi.org/10.1300/J044v07n03_04

Accepted Manuscript/Pre-publication version

629 Tong, Y., Zhu, X., Yan, Y., Liu, R., Gong, F., Zhang, L., Hu, J., Fang, L., Wang, R., & Wang, P.
630 (2015). The influence of different drying methods on constituents and antioxidant activity of
631 saffron from China. *International Journal of Analytical Chemistry*, *2015*, 953164.
632 https://doi.org/10.1155/2015/953164
633 Tsimidou, M., & Biliaderis, C. G. (1997). Kinetic studies of saffron (*Crocus sativus* L.) quality
634 deterioration. *Journal of Agricultural and Food Chemistry, 45*(8), 2890–2898.
635 https://doi.org/10.1021/jf970076n
636 Tzounis, A., Katsoulas, N., Bartzanas, T., & Kittas, C. (2017). Internet of Things in agriculture, recent
637 advances and future challenges. *Biosystems Engineering, 164*, 31–48.
638 https://doi.org/10.1016/j.biosystemseng.2017.09.007
639 Verdouw, C., Tekinerdogan, B., Beulens, A., & Wolfert, S. (2021). Digital twins in smart farming.
640 *Agricultural Systems, 189*, 103046. https://doi.org/10.1016/j.agsy.2020.103046
641 Wolfert, S., Ge, L., Verdouw, C., & Bogaardt, M.-J. (2017). Big data in smart farming – A review.
642 *Agricultural Systems, 153*, 69–80. https://doi.org/10.1016/j.agsy.2017.01.023

Accepted Manuscript/Pre-publication version